

Axial Sensitivity Of A Cracked Probe Of A Scanning Near-Field Optical Microscope

Yu-Ching Yang, Win-Jin Chang, and Haw-Long Lee

Department of Mechanical Engineering /Kun Shan University,
No.195, Kunda Rd., Yong Kang Dist., Tainan City 710-03, Taiwan (R.O.C.)
ycyang@mail.ksu.edu.tw;changwj@msil/ksu.edu.tw;
hawlong@mail.ksu.edu.tw

Abstract -In this paper, the sensitivity of axial vibration for a Scanning near-field optical microscope probe with a crack has been studied. An explicit expression for the sensitivity of axial vibration modes of the cracked probe has been obtained using the relationship between the resonant frequency and contact axial stiffness of the probe and sample. Results show that the sensitivities of the three modes of the cracked probe are higher than those of the probe without crack when the contact axial stiffness is low. When the contact axial stiffness is high, however, the situation is reverse. Therefore, a cracked probe can be used for imaging soft samples such as biological molecules and polymers. In addition, the crack near the free end of probe that leads to a higher sensitivity. This is useful for the design of a highly sensitive probe.

Keywords: Crack probe /Axial sensitivity/Scanning near-field optical microscope (SNOM)

1. Introduction

The scanning near-field optical microscopy (SNOM) has become one of the major proximal probe technologies. SNOM can be used not only to obtain high resolution images beyond the diffraction limit of light but also to fabricate nanometer-scale structures through material removal, modification, and deposition as shown Dereux et al. (2003), Haumann et al. (2005), Girard et al. (2006), Kim et al. (2007) and Tseng (2007). The fiber probe is the key element of the SNOM and can perform various physical thermal sources refer to Kaupp et al.(2001), Kaupp et al. (2006), and Drezet et al. (2007).

In the last few years, many researchers have had a growing interest in studying the flexural and axial sensitivities of vibration modes. For example, Fang et al.(2003) assumed the optical fiber probe had a uniform circular cross-section and studied the dynamic responses of the probe, including the analyses of the cylindrical probe's sensitivity to axial and flexural vibration. They found that each mode had a different mode shape and a different sensitivity, affected by the rigidity of the probe and the surface's properties. Chang et al. (2005) studied the scanning near-field optical microscope with a tapered optical fiber probe's flexural and axial sensitivity to vibration, and found that the flexural and axial sensitivities of the tapered probe were more sensitive than the uniform probe when the contact stiffness was low. However, the situation was reversed when the contact stiffness became higher.

Cracks may be induced in the SNOM's probe due to fabrication process or under service loading. During scanning, cracks will affect the sensitivity of the SNOM. Nevertheless, to our knowledge, there has been no exploring of the vibration behavior of a probe with crack. In this paper, the crack is assumed to exist in the probe and is modeled as an elastic axial spring connecting two undamaged beam segments shown as Morassi (2001). In addition, the effects of crack parameter, and crack location are studied.

2. Analysis

A schematic diagram of a SNOM with an optical fiber probe that is fixed at one end as depicted in Fig. 1. The probe is assumed to have a uniform circular cross section with radius R , its length is L . For

simplifying the problem, the cladding of an optical fiber probe is not taken into account in this paper. The probe interacts with the sample that is modeled by axial spring stiffness, K . In addition, we assume that the probe has a crack at a distance D from the fixed end and an elastic axial spring with spring stiffness K_c is used to simulate the crack and the probe is divided into two segments by the crack shown as Kumar (2009). The governing equation of axial vibration for the probe with a crack can be expressed as

$$EA \frac{\partial^2 U_1}{\partial X^2} = m \frac{\partial^2 U_1}{\partial t^2} \quad 0 \leq X < D \quad (1)$$

$$EA \frac{\partial^2 U_2}{\partial X^2} = m \frac{\partial^2 U_2}{\partial t^2} \quad D < X \leq L \quad (2)$$

where X is the distance along the center of the probe, t is time, $U_1(X,t)$ and $U_2(X,t)$ is the axial displacement of both segments, respectively, and E , A , and m is Young's modulus, cross sectional area and mass per length of the probe, respectively.

The corresponding boundary conditions are

$$U_1(0,t) = 0 \quad (3)$$

$$EA \frac{\partial U_2(L,t)}{\partial X} = KU_2(L,t) \quad (4)$$

Eq.(3) is the condition of the probe end being fixed, and Eq.(4) is the force balance at $X=L$.

According to the continuity conditions in displacement and axial force between two adjacent portions of the probe due to the presence of the longitudinal spring stiffness is obtained by the following jump conditions as[3]

$$K_c[U_1(D,t) - U_2(D,t)] = -EA \frac{\partial U_1}{\partial X} \quad (5)$$

$$\frac{\partial U_1(D,t)}{\partial X} = \frac{\partial U_2(D,t)}{\partial X} \quad (6)$$

In order to find the longitudinal vibration frequency, the following harmonic solution is assumed:

$$U_1(X,t) = W_1(X)e^{i\omega t} \quad (7)$$

$$U_2(X,t) = W_2(X)e^{i\omega t} \quad (8)$$

where ω is the longitudinal frequency.

The dimensionless variables are defined as follows:

$$\begin{aligned} x = X/L, \quad u_1 = W_1/L, \quad u_2 = W_2/L, \quad b = D/L, \\ k_c = K_c L / EA, \quad \beta = \sqrt{\omega^2 m L^2 / EA}, \quad k = KL / EA \end{aligned} \quad (9)$$

where b , and, k_c , denote dimensionless crack location, and spring stiffness parameter of crack,

respectively, β and k are dimensionless longitudinal frequency, and spring stiffness interaction between probe and sample, respectively.

Substituting the harmonic solution given by (7) and (8) into (1) -(6) and using the dimensionless variables given by (9), the governing equations, continuity conditions and associated boundary conditions can be simplified to the following dimensionless forms:

$$\frac{d^2 u_1}{dx^2} + \beta^2 u_1 = 0, \quad 0 \leq x < b \quad (10)$$

$$\frac{d^2 u_2}{dx^2} + \beta^2 u_2 = 0, \quad b \leq x < 1 \quad (11)$$

$$u_1(b) + \frac{1}{k_c} u_1'(b) = u_2(b) \quad (12)$$

$$u_1'(b) = u_2'(b) \quad (13)$$

$$u_1(0) = 0 \quad (14)$$

$$u_2'(1) = k_c u_2(1) \quad (15)$$

Solutions of Eqs.(10) and (11) can be found in the following forms:

$$u_1(x) = A_1 \cos(\beta x) + B_1 \sin(\beta x) \quad (16)$$

$$u_2(x) = A_2 \cos(\beta x) + B_2 \sin(\beta x) \quad (17)$$

Using the continuity conditions Eqs. (12) and (13), the boundary conditions Eqs.(14) and (15), the eigenfunction of longitudinal vibration frequency can be obtained as:

$$F(k, \beta) = (\beta^2 - 2kk_c) \sin(\beta) + \beta^2 \sin(\beta - 2b\beta) - (2k_c + k) \cos(\beta) - k\beta \cos(\beta - 2b\beta) = 0 \quad (18)$$

According to the dimensionless variables $\beta = \sqrt{\omega^2 mL^2 / EA}$ given by Eq. (9), the frequency is obtained and given by

$$f = \frac{\omega}{2\pi} = \frac{\beta}{2\pi \sqrt{mL^2 / EA}} \quad (19)$$

Finally, the dimensionless sensitivity S_a of the cracked SNOM probe can be expressed as follows:

$$S_a = 2\pi \sqrt{mL^2 / EA} \frac{df}{dk} = - \frac{\partial F / \partial k}{\partial F / \partial \beta} \quad (20)$$

where β can be determined from Eq.(18).

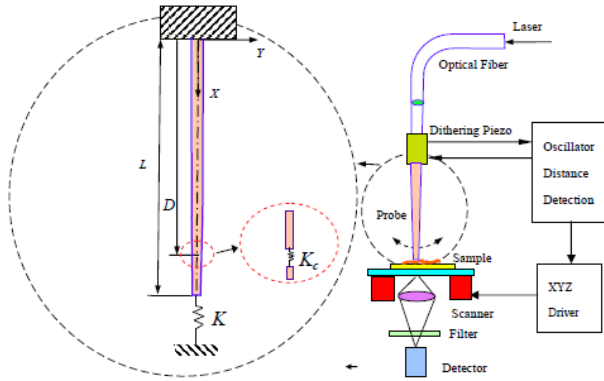


Fig. 1. Schematic diagram of a cracked probe of a SNOM in contact with a sample. The interaction with the sample surface is modeled by axial spring stiffness, K and the crack is modeled as a axial spring stiffness, K_c .

3. Results and Discussion

The main purpose of this paper is to study the effects of crack parameter, and contact axial stiffness on the sensitivity of the vibration modes of a cracked probe of SNOM. The modal sensitivity is defined as the change in the axial frequency of the mode to the change in the tip-sample interaction. In order to know the effect of relative parameters on the sensitivity of a cracked AFM cantilever, we considered the geometric and material parameters as Table.1 shown as Chang (2000). The dimensionless axial sensitivities, S_a , of the first three vibration modes for a cracked probe with $D/L = 0.9$, $k_c = 0.1$ are depicted in Fig. 2. When there is no crack in the probe, it can be seen that the probe is sensitive to changes in the contact stiffness. The low-order vibration modes are more sensitive than the high-order modes when the axial contact stiffness is lower. The first mode was most sensitive. However, when the contact stiffness becomes large, the situation is reversed. These phenomena are the same as those of previous work shown as Chang et al (2005). The cantilever becomes less stiff due to the presence of a crack and that affects its sensitivity. Therefore, the sensitivities of the three modes of the cracked cantilever are larger than those of the cantilever without crack when the normal contact stiffness is low. However, the situation is reverse when the contact stiffness becomes large. This is because a soft cantilever is suitable for imaging soft samples. In addition, the crack effect on the sensitivity is more significant for the higher-order modes.

The dimensionless sensitivity of mode 1 as functions of crack location and axial contact stiffness for the probe is illustrated in Figure 3. The elastic energy of a cracked probe during scanning obviously decreases as the crack is close to the free end. The crack near the free end shows significant changes in the frequency. Therefore, the sensitivity is high for a larger value of D/L .

The crack parameter indicates crack configuration and crack depth and is related to the changes of natural frequency and sensitivity of cantilever. The dimensionless axial sensitivity of mode 1 as functions of axial contact stiffness and crack parameter for the SNOM's probe is depicted in Figure 4. A crack makes the probe locally less stiff because of the added flexibility. Therefore, the sensitivity of the cracked probe increases with increasing value of crack parameter when the contact stiffness is low. However, when the contact stiffness becomes large, the situation is reverse. It implies that a lower sensitivity is obtained for a softer cantilever scanning a stiffer surface.

Table. 1. Parameters for an optical fiber SNOM probe.

Young's modulus E (GPa)	72.5
Density ρ (g/cm ³)	2.2
Probe length L (μ m)	1500
Cylinder radius R (μ m)	62.5

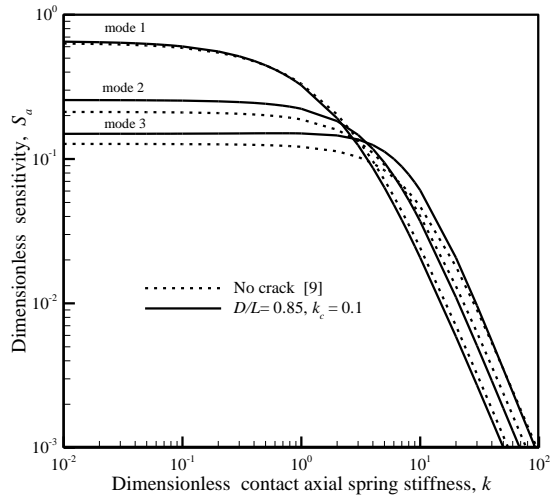


Fig. 2. The crack effect on the dimensionless sensitivity as a function of contact axial stiffness.

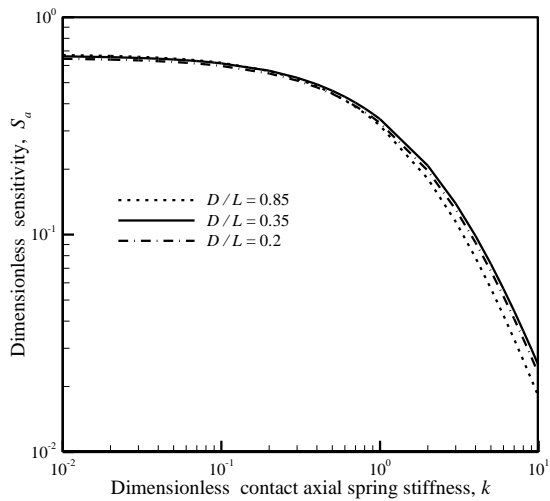


Fig. 3. Dimensionless axial sensitivity of mode 1 as functions of crack location and axial contact stiffness for the SNOM's probe with $k_c = 0.1$.

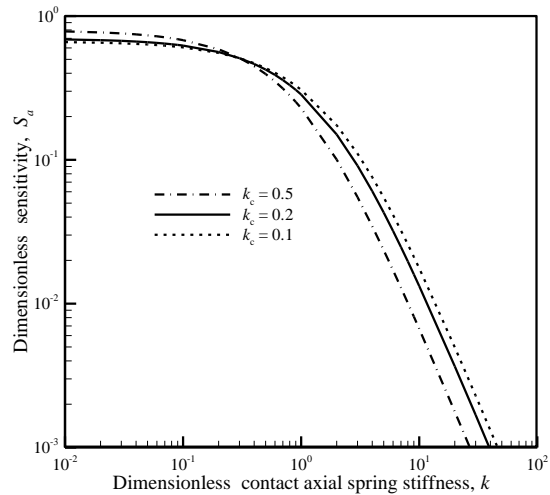


Figure 4. Dimensionless axial modal sensitivity of mode 1 as functions of axial contact stiffness and crack parameter for the SNOM's probe with $D/L=0.85$.

4. Conclusion

In this paper, the effects of crack parameter, and crack location on the axial sensitivity of a probe of SNOM have been analyzed. According to the analysis, the following results are obtained:

1. When the contact axial stiffness is low, the sensitivities of the three modes of the cracked probe were larger than those of the probe without crack. When the contact axial stiffness becomes large, however, the situation was reverse.
2. The crack effect on the sensitivity was more significant for the higher-order modes.
3. The crack was closed to the free end of cantilever that made a higher modal sensitivity.
4. When the contact axial stiffness was low, the sensitivity of the cracked probe increased with increasing value of crack parameter. However, the situation was reverse when the contact axial stiffness became large.

Acknowledgements

This work was supported by the Ministry of Science and Technology, Taiwan, Republic of China, under the grant number MOST 103-2221-E-168-014.

References

- Dereux, A., Girar, C. D., Chicanne, C., Colas, F. G., David, T., Bourillot, E., Lacrou, Y. E., & Weeber, J. (2003). Subwavelength Mapping Of Surface Photonic States. *Nanotechnology*, 14, 935.
- Haumann, C., Pelargus, Ch., Frey, H. G., Ros, R., Anselmetti, D., Toquant, J., & Pohl, D. W. (2005). Stand-Alone Device For The Electrolytic Fabrication Of Scanning Near-Field Optical Microscopy Aperture Probes. *Rev. Sci. Instrum.*, 76, 033704.
- Girard, C., & Dujardin, E. (2006). Near-Field Optical Properties Of Top-Down And Bottom-Up Nanostructures. *J. Opt. A: Pure Appl.*, S73.
- Kim, J. H., & Song, K. B. (2007). Recent Progress Of Nano-Technology With NSOM Micron, 38, 409.
- Tseng, A. A. (2007). Recent Developments In Nanofabrication Using Scanning Near-Field Optical Microscope Lithography. *Opt. Laser Technol.*, 39, 514.
- Kaupp, G., Herrmann, A., Schmeyers, J., & Boy, J. (2001). SNOM: A New Photophysical Tool. *J. Photoch. Photobio. A*, 139, 93.
- Kaupp, L., Samson, B., Julié, G., Mathet, V., Lequeu, N. X., Allen, C. N., Diaf, H., & Dubertret, B. (2006). Scanning Near-Field Optical Microscope Working With A Quantum Dot Based Optical Detector. *Rev. Sci. Instrum.*, 77, 063702.
- Drezet, A., Hohenau, A., Krenn, J. R., Brun, M., & Huan, S. T. (2007). Surface Plasmon Mediated Near-Field Imaging And Optical Addressing In Nanoscience. *Micron*, 38, 427.
- Fang, T. H., & Chang, W. J. (2003). Sensitivity Analysis Of Scanning Near-Field Optical Microscope Probe. *Opt. Laser Technol.*, 35, 267.
- Chang, W. J., Fang, T. H., Lee, H. L., & Yang, Y. C. (2005). Vibration Sensitivity Of The Scanning Near-Field Optical Microscope With A Tapered Optical Fiber Probe. *Ultramicroscopy*, 102, 85.
- Morassi, A., (2001). Identification Of A Crack In A Rod Based On Changes In A Pair Of Natural Frequencies. *J. Sound Vib.*, 242 577.
- Kumar, V. S. (2009). Transcendental Inverse Eigenvalue Problems In Damage Parameter Estimation. *Mechanical Systems and Signal Processing*, 23, 1870–1883. Retrieved from doi:10.1016/j.ymssp.2008.05.009
- Chang, W. J., Lee, H. L., & Yang, Y. C. (2000). Hydrostatic Pressure And Thermal Loading Induced Optical Effects In Double-Coated Optical Fibers. *J Appl. Phys.*, 88(2), 616–20.